

# 100-300GHz Wireless: ICs, Arrays, and Systems

M. J. W. Rodwell<sup>1</sup>, Ali A. Farid<sup>1</sup>, A. S. H. Ahmed<sup>1</sup>, M. Seo<sup>2</sup>, U. Soyulu<sup>1</sup>, A. Alizadeh<sup>1</sup>, N. Hosseinzadeh<sup>1</sup>,

<sup>1</sup>Department of Electrical and Computer Engineering University of California, Santa Barbara, USA

<sup>2</sup>Department of Electrical and Computer Engineering, Sungkyunkwan University, South Korea  
rodwell@ece.ucsb.edu

**Abstract**— 100-300GHz wireless systems can provide very high data rates per signal beam, and, given the short wavelengths, even compact arrays can contain many elements, and hence can simultaneously transmit, in the same frequency band, many simultaneous independent signal beams to further greatly increase capacity. We will describe representative system designs, including wireless hubs and wireless backhaul links using massive spatial multiplexing, plus imaging radar systems, evaluate their feasible performance, and identify the key challenges in implementation, including transistor and IC performance, array physical design, digital beam former complexity, and systems cost.

**Keywords**—*mm-wave wireless, 6G wireless, mm-wave ICs, THz wireless, mm-wave MIMO.*

## I. INTRODUCTION

Rapidly increasing use of wireless communications is exhausting the presently allocated spectrum, hence the wireless industry is moving to 5G wireless systems, with carrier frequencies ranging from sub-6GHz to 86GHz. Research now considers next-generation systems with carrier frequencies between 100-300GHz. Capacity can be further increased over 5G, both because of the wide potentially available spectrum and because the short wavelengths permit compact arrays having many elements which can then support many simultaneous independent signal beams, this being known as massive spatial multiplexing or massive MIMO. Simple link budget analyses suggest that, with present state-of-the-art power- and low-noise amplifiers, aggregate capacities can approach or exceed 1Tb/s in short-range (few hundred meter) backhaul and endpoint links. The challenges in realizing such systems are in efficient digital beamforming, in the array physical design, and in realizing the front-end ICs and modules at low power consumption and low cost, particularly given the large number of required RF channels.

## II. 100-300GHz WIRELESS SYSTEMS

Consider first [1, 2] a 140GHz wireless communications hub (base station) serving many mobile users (Figure 1). Each array face has 32 elements and supports 16 users but is only 41mm long. If we assume that the hub's power amplifiers each provide 120mW at the 1dB gain compression point, that the handset has a 1cm<sup>2</sup> array (8×8 at  $\lambda/2$  spacing) and has 8dB noise figure, that it is raining 50mm/hr., and that the signaling is QPSK at 10<sup>-3</sup> uncoded error rate, then the hub can provide each user with 1Gb/s (10Gb/s) data rate at 110m (40m) range, even with 17dB total safety margins for partial beam blockage, equipment aging, and manufacturing variations. The net transmission capacity is 160Gb/s per array face. If we assume

the same link parameters at 75GHz, keep the base station at 32 elements, but constrain the handset array to the same 1cm<sup>2</sup> area (4×4 elements at  $\lambda/2$  spacing) as at 140GHz, then the same range is obtained at the same data rate; at 140GHz, it is more likely that the needed spectrum can be allocated.

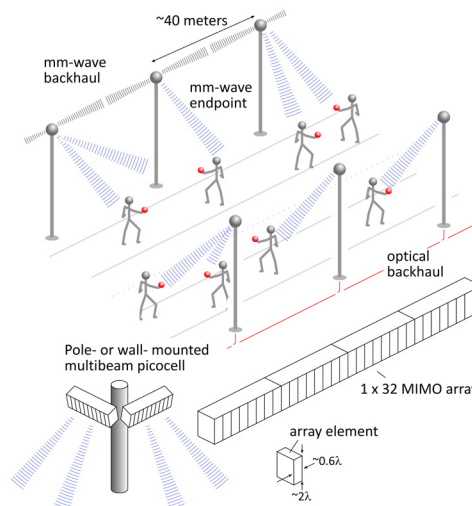


Figure 1: Spatially multiplexed network 140GHz picocell hub. The hub has 2 faces, each a 32-element MIMO array, each providing up to 16 independent signal beams. At 40m range, 10Gb/s transmission per beam is feasible with large operating margins.

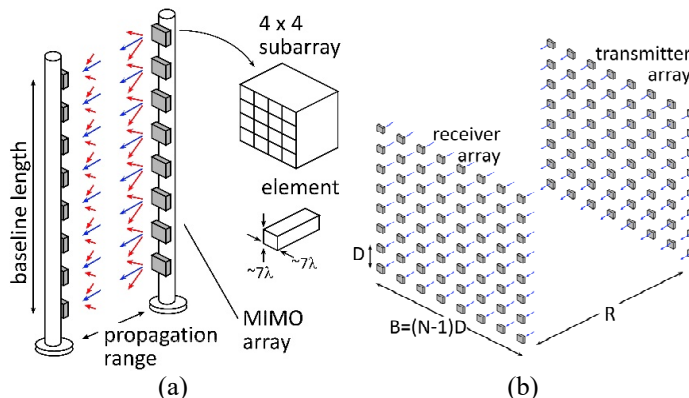


Figure 2: Spatially multiplexed wireless backhaul link, using (a) linear transmitter and receiver arrays, with each element being a 4×4 subarray. With a fixed range and baseline length, the maximum number of channels scales in proportion to the carrier frequency. Spatially multiplexed link using (b) a square array, with the number of channels scaling in proportion to the square of the carrier frequency.

Figure 2a shows a spatially multiplexed backhaul link.  $N$  transmitters, carrying independent data, form an array of length

$L$ . The receiver, at distance  $R$ , has a similar array but uses MIMO [3] beamforming. If the array angular resolution  $\lambda/L$  is smaller than the element apparent angular separation  $L/NR$ , then the signals can be recovered without channel-channel crosstalk degrading the SNR. Link capacity is increased  $N:1$ . In a square array (Figure 2b), the capacity is increased  $N^2:1$ .

Short wavelengths are of great advantage, as a short array can then carry many channels; at 500m range, an 8-element linear array must be 2.1m long at 210GHz, but 3.5m at 75GHz. At 210GHz, if each array element is an  $8 \times 8$  subarray of  $7\lambda$  by  $7\lambda$  elements (for small beam angle adjustment) then, with 20 dB total margins, QPSK at  $10^{-3}$  uncoded error rate, and 6dB receiver noise figure, transmitting 640Gb/s over 500m range in 50mm/hr. rain requires only 63 mW/element output power at the 1dB gain compression point. Given the same system parameters, the square array would transmit 5.1Tb/s but would require only 8 mW/element output power ( $P_{1dB}$ ).

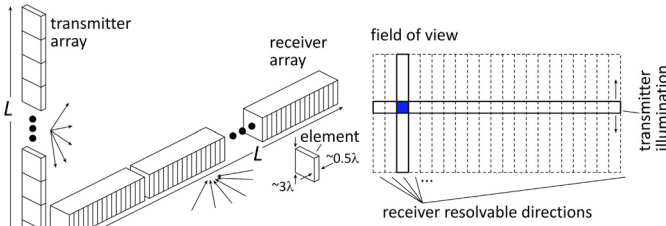


Figure 3: Automotive imaging radar system using a  $N \times 1$  vertical linear phased-array transmitter and a  $1 \times N$  horizontal linear MIMO array receiver to produce an  $N \times N$  image.

A third example system (Figure 3) is a 210GHz FMCW imaging radar, for driving in e.g. heavy fog or rain. Crossed linear  $36 \times 1$  transmit and  $1 \times 216$  receive arrays form a  $36$  (vertical)  $\times$   $216$  (horizontal) pixel image. If the elements are  $3\lambda$  (v)  $\times$   $0.5\lambda$  (h), then the array length  $L$  is only 15.3cm, yet the 3dB beamwidth is  $0.27^\circ$ , while the field of view is  $10^\circ$  (v)  $\times$   $90^\circ$  (h). Given a 40Hz image scan rate, a 22cm diameter target (a soccer ball) of -10dB reflectivity at 200m range, a minimum 10dB SNR for target detection, 22dB/km atmospheric attenuation (heavy fog or 50mm/hr. rain), and 4 dB operating margins, then with 2dB transmit and 2dB receive packaging losses and a 6dB receiver noise figure, the required transmitter output power per element is 50mW.

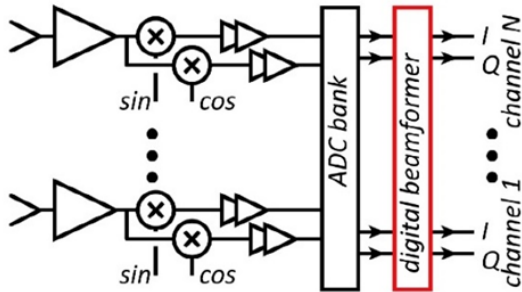


Figure 4: Sketch of the RF through baseband signal chain, with digital beamforming, for the massive MIMO receiver of Figure 1. The transmitter is similar, with digital beam former, DAC bank, (I,Q) baseband to RF up conversion, power amplifiers, and antennas..

### III. SIGNAL PROCESSING REQUIREMENTS

The MIMO systems considered above collectively carry many high-rate signal streams, hence signal-signal crosstalk from RF/IF/baseband signal chain (Figure 4) nonlinearities ( $P_{1dB}$ , IP3), ADC/DAC resolution, and local oscillator phase noise are of potential concern. Yet, detailed systems simulations of the MIMO hub of Figure 1 indicate that, if received power leveling is employed, RF component 1dB gain compression points need only be 4dB above average power levels [4], that 3-4 bit ADC/DAC resolution is sufficient for QPSK transmission [4], and that the phase noise need be no smaller than that required of a single-channel system of the same symbol rate and constellation [5]. These findings suggest that the design requirements of the RF, IF, and baseband analog ICs are not particularly stringent. Given that  $\sim 16$  high-rate (1-10Gb/s) user data streams must be recovered from  $\sim 32$  wideband (I,Q) signals, the digital beam former might potentially be very computationally complex. Yet, with the development of computationally efficient beam space beamforming algorithms [6] and efficient VLSI digital implementations [7], high-rate all-digital MIMO beamforming appears to be feasible.

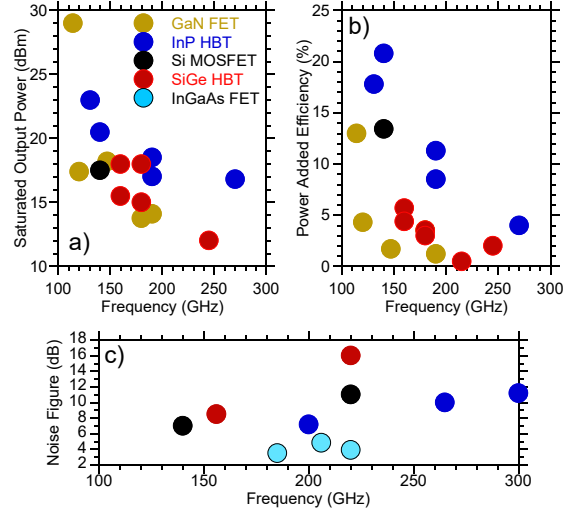


Figure 5: Representative state-of-the-art results at 100-300GHz for power amplifier saturated output power (a) and power-added-efficiency (b) and receiver or LNA noise figure (c). Because it is difficult to simultaneously present power amplifier operating frequency, output power, and efficiency, results with very low efficiency but high output power, or low output power but high efficiency are not shown.

### IV. IC TECHNOLOGIES FOR 100-300GHZ WIRELESS

Even today's IC technologies (Figure 5) can provide the frequency range, transmitter power and receiver noise required for the systems of figures 1-3; the challenge is in either realizing the ICs in lower-cost CMOS and SiGe technologies, or, if higher-performance InP or GaN [8, 9, 10] technologies are to be used, in bringing these to low cost and high production volumes. CMOS works well at 140-150GHz, [11,12] providing low receiver noise and moderate output power [13,14]; 140GHz arrays have been reported [13,15], but receiver noise and power amplifier output power and efficiency

degrade markedly at higher frequencies [16]. Best CMOS performance at 100-200GHz is for the 65nm through 32nm nodes, not more highly scaled technologies. Longer-range ~150GHz wireless links can use CMOS with external InP HBT [17,18, 19, 20] or SiGe HBT power amplifiers [21,22,23] for increased output power; InP, in particular, provides record power and efficiency at these frequencies. InP HEMT or GaAs PHEMT or MHEMT low-noise amplifiers can be used for better receiver sensitivity [24,25,26]. For systems having >200GHz carrier frequencies, though CMOS can still be used for frequency conversion [27,28], for best IC performance, and to reduce the number of high-frequency IC-IC connections, it may be attractive to build the entire RF front end from III-V or SiGe technologies. Figure 6 shows some representative ICs, including full 200GHz transmitters and receivers [29] intended for MIMO backhaul links (Figure 2).

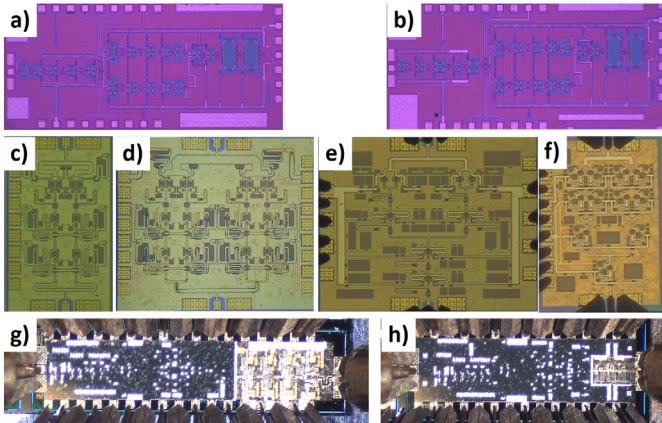


Figure 6: Representative 100-300GHz ICs, including a 140GHz receiver (a) and transmitter (b) in 22nm SOI CMOS, InP HBT power amplifiers at (c) 140GHz with 109mW power and 20.8% PAE, (d) 131GHz with 200mW power and 17.8% PAE, (e) 194GHz with 55mW power and 8.5% PAE, and (f) 266GHz with 48mW power and 4% PAE, and (g) a 200GHz transmitter with 34mW output power, and (h) a 200GHz receiver with 7.7-9.3dB noise figure, both in 250nm InP HBT.

## V. ARRAY MODULE DESIGN

100-300GHz array transceivers present significant packaging challenges. To steer over 180° both in azimuth and elevation, the array must be 2-dimensional and must have  $\sim\lambda/2$  element spacing,  $\sim 1\text{mm}$  at 140GHz and  $0.5\text{mm}$  at 300GHz. It is difficult to fit the necessary RF electronics in a small available area, and it can be difficult to remove the heat, particularly if inefficient or high-power PAs are used.

If the users are mostly distributed over the ground, then the array is best designed to steer only in azimuth, and is then 1-dimensional (Figure 1). There is then sufficient space along the edges of the array both to fit the mm-wave front-end ICs and to remove the heat. Figure 7 shows an 8-channel transmitter array tile module designed 140GHz MIMO hubs (Figure 1). Experiments with these are in progress [30].

In MIMO backhaul links (Figure 2), phased-array beam steering in two planes over a small angular range can correct for small angular aiming errors from installation. For 10° beam steering range, the elements can be spaced at  $\sim 7\lambda$ . Figure 8

shows an array tile design for this application, with linear arrays of antennas and ICs mounted on a metal tray, with trays then stacked to form a 2D array. We are presently developing versions of these modules both at 200GHz using previously-designed ICs [29] and at 280GHz using ICs now in development.

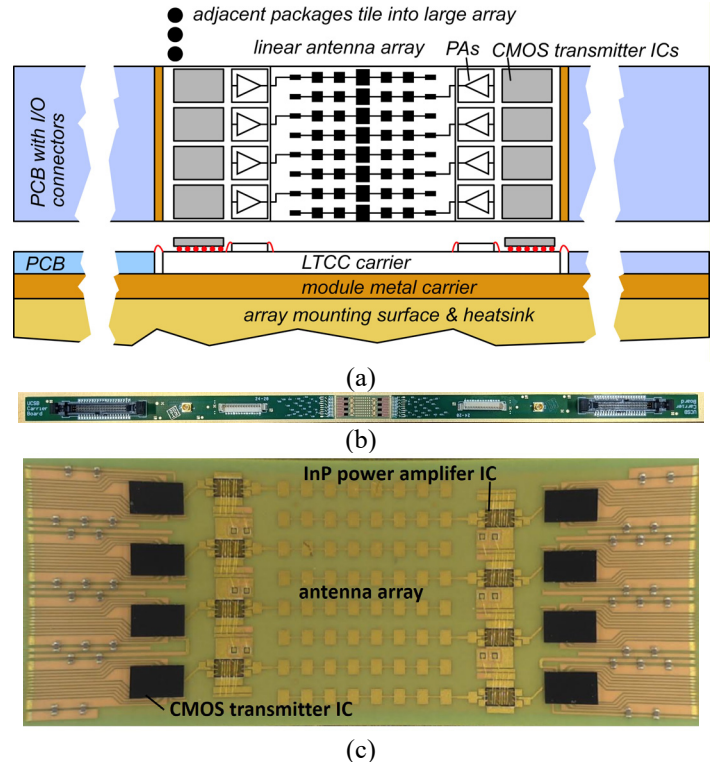


Figure 7: Eight-channel 140GHz MIMO hub transmitter array tile module: (a) schematic cross-section diagram showing the interface printed circuit boards, the LTCC carrier, connectors, and ICs, (b) photograph of the overall module, and (c) photograph of the LTCC carrier showing the antennas and CMOS and InP ICs. The overall module is  $450\text{mm} \times 15\text{mm}$ , while the LTCC carrier is approximately  $12\text{mm} \times 33\text{mm}$

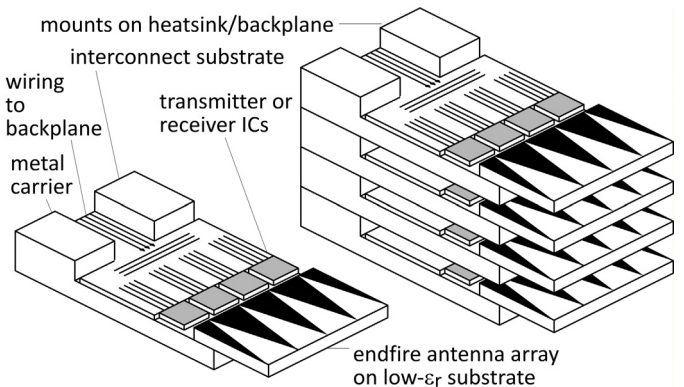


Figure 8: Array tile design with  $\sim 7\lambda$  spacing for small-angular-deviation 2D beam steering in fix-aimed point-point links.

## VI. CONCLUSIONS

A wide radio spectrum is available between 100GHz and 300GHz; further, because the wavelengths are short, massive spatial multiplexing is feasible even from compact arrays.

Aggregate capacities in endpoint and backhaul links can approach or even exceed 1Tb/s, but high atmospheric losses limit range to 100-500m. Challenges include digital beamforming, array module packaging, and the cost and power consumption of the mm-wave arrays, these containing many elements.

#### ACKNOWLEDGMENTS

This work was supported in part by the Semiconductor Research Corporation and DARPA under the JUMP program. The authors thank Kyocera for fabrication of the LTCC carriers and module assembly and GlobalFoundries for 22nm FDSOI IC fabrication and for free access to advanced copper pillars. Thanks to Gary Xu and Navneet Sharma of Samsung Research America for guidance and encouragement.

#### REFERENCES

- [1] M. J. W. Rodwell et al., "100-340GHz Systems: Transistors and Applications," 2018 IEEE International Electron Devices Meeting (IEDM), 2018, pp. 14.3.1-14.3.4, doi: 10.1109/IEDM.2018.8614537.
- [2] M. J. W. Rodwell, "100-340GHz Spatially Multiplexed Communications: IC, Transceiver, and Link Design," 2019 IEEE 20th International Workshop on Signal Processing Advances in Wireless Communications (SPAWC), 2019, pp. 1-5, doi: 10.1109/SPAWC.2019.8815433.
- [3] C. Sheldon, M. Seo, E. Torkildson, M. Rodwell and U. Madhow, "Four-channel spatial multiplexing over a millimeter-wave line-of-sight link," 2009 IEEE International Microwave Symposium, Boston, MA, doi: 10.1109/MWSYM.2009.5165715.
- [4] M. Abdelghany, A. A. Farid, M. E. Rasekh, U. Madhow and M. J. W. Rodwell, "A design framework for all-digital mmWave massive MIMO with per-antenna nonlinearities," in IEEE Transactions on Wireless Communications, doi: 10.1109/TWC.2021.3069378.
- [5] M. E. Rasekh, M. Abdelghany, U. Madhow and M. Rodwell, "Phase noise analysis for mmwave massive MIMO: a design framework for scaling via tiled architectures," 2019 53rd Annual Conference on Information Sciences and Systems (CISS), 2019, pp. 1-6, doi: 10.1109/CISS.2019.8693033.
- [6] M. Abdelghany, U. Madhow and A. Tölli, "Beamspace Local LMMSE: An Efficient Digital Backend for mmWave Massive MIMO," 2019 IEEE 20th International Workshop on Signal Processing Advances in Wireless Communications (SPAWC), 2019, pp. 1-5, doi: 10.1109/SPAWC.2019.8815585.
- [7] O. F. Castaneda Fernandez, Z. Boynton, S. H. Mirfarshbafan, S. Huang, J. Ye, A. Molnar, C. Studer, "A Resolution-Adaptive 8mm2 9.98Gb/s 39.7pJ/b 32-Antenna All-Digital Spatial Equalizer for mmWave Massive MU-MIMO in 65nm CMOS", 2021 European Solid-state Circuits and Devices Conference, Grenoble, September (online).
- [8] M. Ćwikliński et al., "190-GHz G-Band GaN Amplifier MMICs with 40GHz of Bandwidth," 2019 IEEE MTT-S International Microwave Symposium (IMS), 2019, pp. 1257-1260, doi: 10.1109/MWSYM.2019.8700762.
- [9] A. Margomenos et al., "GaN Technology for E, W and G-Band Applications," 2014 IEEE Compound Semiconductor Integrated Circuit Symposium (CSICS), 2014, pp. 1-4, doi: 10.1109/CSICS.2014.6978559.
- [10] A. Fung et al., "Gallium nitride amplifiers beyond W-band," 2018 IEEE Radio and Wireless Symposium (RWS), 2018, pp. 150-153, doi: 10.1109/RWS.2018.8304971.
- [11] A. Simsek, S. Kim and M. J. W. Rodwell, "A 140 GHz MIMO Transceiver in 45 nm SOI CMOS," 2018 IEEE BiCMOS and Compound Semiconductor Integrated Circuits and Technology Symposium (BCICTS), 2018, pp. 231-234, doi: 10.1109/BCICTS.2018.8550954.
- [12] A. A. Farid, A. Simsek, A. S. H. Ahmed and M. J. W. Rodwell, "A Broadband Direct Conversion Transmitter/Receiver at D-band Using CMOS 22nm FDSOI," 2019 IEEE Radio Frequency Integrated Circuits Symposium (RFIC), 2019, pp. 135-138, doi: 10.1109/RFIC.2019.8701730.
- [13] S. Li, Z. Zhang, B. Rupakula, G. M. Rebeiz, "An Eight-Element 140-GHz Wafer-Scale IF Beamforming Phased-Array Receiver with 64-QAM Operation in CMOS RFSOI" *in review*.
- [14] S. Li, G. M. Rebeiz, "A 130-151 GHz 8-Way Power Amplifier with 16.8-17.5 dBm Psat and 11.7-13.4% PAE Using CMOS 45nm RFSOI", 2021 IEEE RFIC Symposium, June.
- [15] S. Li, G. Rebeiz, "An Eight-Element 140GHz Wafer-Scale Phased-Array Transmitter with 32dBm Peak EIRP and >16Gbps 16QAM and 64QAM Operation", IEEE International Microwave Symposium (IMS), 6-11 June, Atlanta and virtual.
- [16] M. Varonen A. Safaripour D. Parveg P. Kangaslahti T. Gaier A. Hajimiri, "200 - GHz CMOS amplifier with 9 - dB noise figure for atmospheric remote sensing", Electronics Letters, Volume 52, Issue 5, March 2016, Pages 369-371
- [17] A. S. H. Ahmed, M. Seo, A. A. Farid, M. Urteaga, J. F. Buckwalter and M. J. W. Rodwell, "A 140GHz power amplifier with 20.5dBm output power and 20.8% PAE in 250-nm InP HBT technology," 2020 IEEE/MTT-S International Microwave Symposium (IMS), 2020, pp. 492-495, doi: 10.1109/IMS30576.2020.9224012.
- [18] A. S. H. Ahmed, M. Seo, A. A. Farid, M. Urteaga, J. F. Buckwalter and M. J. W. Rodwell, "A 200mW D-band Power Amplifier with 17.8% PAE in 250-nm InP HBT Technology," 2020 15th European Microwave Integrated Circuits Conference (EuMIC), 2021, pp. 1-4, doi: 10.1109/EuMIC48047.2021.00012.
- [19] A. S. H. Ahmed, U. Soyly, M. Seo, M. Urteaga, M. J. W. Rodwell, "A 190-210GHz Power Amplifier with 17.7-18.5dBm Output Power and 6.9-8.5% PAE", IEEE International Microwave Symposium (IMS), 6-11 June, Atlanta and virtual.
- [20] A. S. H. Ahmed, U. Soyly, M. Seo, M. Urteaga, M. J. W. Rodwell, "A compact H-band Power Amplifier with High Output Power", IEEE Radio-Frequency IC Symposium (IMS), 7-9 June, Atlanta and virtual
- [21] M. Furqan, F. Ahmed, B. Heinemann and A. Stelzer, "A 15.5-dBm 160-GHz High-Gain Power Amplifier in SiGe BiCMOS Technology," in IEEE Microwave and Wireless Components Letters, vol. 27, no. 2, pp. 177-179, Feb. 2017, doi: 10.1109/LMWC.2016.2646910.
- [22] M. H. Eissa and D. Kissinger, "4.5 A 13.5dBm Fully Integrated 200-to-255GHz Power Amplifier with a 4-Way Power Combiner in SiGe:C BiCMOS," 2019 IEEE International Solid-State Circuits Conference - (ISSCC), 2019, pp. 82-84, doi: 10.1109/ISSCC.2019.8662424.
- [23] A. Ali, J. Yun, F. Giannini, H. J. Ng, D. Kissinger and P. Colantonio, "168-195 GHz Power Amplifier With Output Power Larger Than 18 dBm in BiCMOS Technology," in IEEE Access, vol. 8, pp. 79299-79309, 2020, doi: 10.1109/ACCESS.2020.2990681.
- [24] C. M. Cooke et al., "A 220 GHz Dual Channel LNA Front-End for a Direct Detection Polarimetric Receiver," 2019 IEEE MTT-S International Microwave Symposium (IMS), 2019, pp. 508-511, doi: 10.1109/MWSYM.2019.8701101.
- [25] G. Moschetti et al., "A 183 GHz Metamorphic HEMT Low-Noise Amplifier With 3.5 dB Noise Figure," in IEEE Microwave and Wireless Components Letters, vol. 25, no. 9, pp. 618-620, Sept. 2015, doi: 10.1109/LMWC.2015.2451355.
- [26] A. Tessmann, A. Leuther, H. Massler, M. Kuri and R. Loesch, "A Metamorphic 220-320 GHz HEMT Amplifier MMIC," 2008 IEEE Compound Semiconductor Integrated Circuits Symposium, 2008, pp. 1-4, doi: 10.1109/CSICS.2008.12.
- [27] I. Momson, S. Lee, S. Dong and K. O., "425-to-25-GHz CMOS-Integrated Downconverter," in IEEE Solid-State Circuits Letters, vol. 4, pp. 80-83, 2021, doi: 10.1109/LSSC.2021.3067192.
- [28] S. Kang, S. V. Thyagarajan and A. M. Niknejad, "A 240 GHz Fully Integrated Wideband QPSK Transmitter in 65 nm CMOS," IEEE Journal of Solid-State Circuits, vol. 50, no. 10, pp. 2256-2267, Oct. 2015, doi: 10.1109/JSSC.2015.2467179.
- [29] M. Seo, A. S. H. Ahmed, U. Soyly, A. Farid, Y. Na, M. Rodwell, "A 200 GHz InP HBT Direct-Conversion LO-Phase-Shifted Transmitter/Receiver with 15 dBm Output Power" IEEE International Microwave Symposium (IMS), 6-11 June, Atlanta and virtual
- [30] A. Farid, A. S. H. Ahmed, A. Simsek, M. J. W. Rodwell, "A 27.5dBm EIRP D-Band Transmitter Module on a Ceramic Interposer", IEEE Radio-Frequency IC Symposium (IMS), 7-9 June, Atlanta and virtual